Interaction of Alcohols and Ethers with *a*-CF_x Films

Min Soo Lim, Yang Yun, and Andrew J. Gellman*

Department of Chemical Engineering, Carnegie Mellon University, Pittsburgh, Pennsylvania 15213

Received July 5, 2005. In Final Form: October 10, 2005

The surfaces of the magnetic data storage hard disks used in computers are coated with a thin film of amorphous carbon and a layer of perfluoropolyalkyl ether (PFPE) lubricant. Both protect the surface of the magnetic layer from contact with the read−write head flying over the disk surface. Although the most commonly used carbon films are amorphous hydrogenated carbon, *a*-CH_x, it has been suggested that the thermal properties of amorphous fluorinated carbon films, *a*-CF_x, might be superior. This work has probed the interaction of small fluorinated ethers and alcohols with the surfaces of *a*-CF_x films to understand the effects of carbon film fluorination on the interaction of the lubricant with its surface. Temperature-programmed desorption was used to measure the desorption energies of small fluorocarbons from the *a*-CF_x surface and to compare their desorption energies with those from the surfaces of *a*-CH_x films. These measurements reveal that, similarly to *a*-CH_x films, *a*-CF_x films expose a heterogeneous surface on which fluorocarbons adsorb at sites with a range of binding energies. The fluorocarbon ethers all have lower heats of adsorption than their hydrocarbon counterparts, suggesting that the ethers adsorb by donation of electron density from the oxygen lone-pair electrons to sites on the surface. Fluorinated alcohols have roughly the same heats of adsorption as their hydrocarbon counterparts. There is little significant difference between the interactions of fluorinated ethers (or alcohols) with the surfaces of either *a*-CF_x or *a*-CH_x films.

1. Introduction

Magnetic recording has been the primary data recording technology for the past 40 years because it provides fast and cheap random access to large amounts of data. In hard disk drives, data is written to and read from a rotating disk that is coated with a thin magnetic film. This magnetic film, which serves as the recording and storage medium, is protected by a thin carbon overcoat with a thickness of less than 100 Å and a polymeric liquid lubricant film with a thickness of 5−20 Å. These minimize friction at the head−disk interface (HDI) and provide wear resistance during intermittent, high-speed contacts between the read−write head and the disk surface.[1,2]

The areal storage density (the number of data bits stored per unit area) of hard disk drives has been increasing continuously for the past decade at rates as high as 100% per year and has now reached densities in excess of 100 Gbits/in.[3,4] Increases in areal density are achieved partly by reducing the head−disk space, which is now approaching the atomic scale (<100 Å).[5] Further reduction of the head−disk space will cause more frequent high-speed contact of the read−write head with the disk surface, eventually leading to hard disk failure. Consequently, new materials with better tribological and mechanical performances are required for use as protective coatings for the underlying magnetic layer. Amorphous hydrogenated carbon (*a*-CH_x) overcoats have been used to protect conventional hard disks because of their hardness and their ability to provide wear and corrosion protection.[6] It has been proposed that fluorine incorporation in the carbon overcoat might improve its tribological and nonwetting properties while maintaining mechanical properties comparable to those of *a*-CH_x films.[7−10]

Fluorinated amorphous carbon (*a*-CF_x) films have been produced by plasma-enhanced chemical vapor deposition (PECVD),[7,11−26] inductively coupled plasma chemical vapor

* Corresponding author. E-mail: gellman@cmu.edu.

(1) Mate, C. M. Molecular tribology of disk drives. *Tribol. Lett.* **1998**, *4* (2), 119−123.

(2) Gellman, A. J. Lubricants and overcoats for magnetic storage media. *Curr. Opin. Colloid Interface Sci.* **1998**, *3* (4), 368−372.

(3) Zhu, Y.-L.; Liu, B.; Li, Y.-H.; Leng, Q.-F. Slider−disk interaction and its effect on the flying performance of slider. *IEEE Trans. Magn.* **1999**, *35* (5), 2403−2405.

(4) Thomson, D. A.; Best, J. S. The future of magnetic data storage technology. *IBM J. Res. Dev.* **2000**, *44* (3), 311−321.

(5) Zhu, J.-G. New heights for hard disk drives. *Mater. Today* **2003**, *6* (7/8), 22−31.

(6) Tsai, H.-C.; Bogy, D. B. Critical review: Characterization of diamondlike carbon films and their application as overcoats on thin-film media for magnetic recording. *J. Vac. Sci. Technol. A* **1987**, *5* (6), 3287−3312.

(7) Freire, F. L., Jr.; Maia da Costa, M. E. H.; Jacobsohn, L. G.; Franceschini, D. F. Film growth and relationship between microstructure and mechanical properties by PECVD. *Diamond Relat. Mater.* **2001**, *10*, 125−131.

(8) Hakovirta, M.; Lee, D. H.; He, X. M.; Nastasi, M. Synthesis of fluorinated diamond-like carbon films by the plasma immersion ion processing technique. *J. Vac. Sci. Technol. A* **2001**, *19* (3), 782−784.

(9) Hakovirta, M.; Verda, R.; He, X. M.; Nastasi, M. Heat resistance of fluorinated diamond-like carbon films. *Diamond Relat. Mater.* **2001**, *10*, 1486−1490.

(10) Jacobsohn, L. G.; Maia da Costa, M. E. H.; Triva-Airoldi, V. J.; Freire, F. L., Jr. Hard amorphous carbon−florine films deplosited by PECVD using C_2H_2−CF_4 gas mixture as precursor atmospheres. *Diamond Relat. Mater.* **2003**, *12*, 2037−2041.

(11) Shieh, J.-M.; Tsai, K.-C.; Dai, B.-T.; Wu, Y.-C.; Wu, Y.-H. Reduction of etching plasma damage on low dielectric constant fluorinated amorphous carbon films by multiple H_2 plasma treatment. *J. Vac. Sci. Technol. B* **2002**, *20* (4), 1476−1481.

(12) Shieh, J.-M.; Tsai, K.-C.; Dai, B.-T.; Lee, S.-C.; Ying, C.-H.; Fang, Y.-K. Modifications of Low Dielectric Constant Fluorinated Amorphous Carbon Films by Multiple Plasma Treatments. *J. Electrochem. Soc.* **2002**, *149* (7), G384−G390.

(13) Wang, X.; Harris, H. R.; Bouldin, K.; Temkin, H.; Gangopadhyay, S. Structural properties of fluorinated amorphous carbon films. *J. Appl. Phys.* **2000**, *87* (1).

(14) Theil, J. A. Fluorinated amorphous carbon films for low permittivity interlevel dielectrics. *J. Vac. Sci. Technol. B* **1999**, *17* (6), 2397−2410.

(15) Endo, K.; Shinoda, K.; Tatsumi, T. Plasma deposition of low-dielectric-constant fluorinated amorphous carbon. *J. Appl. Phys.* **1999**, *86* (5), 2739−2745.

(16) Yang, H.; Tweet, D. J.; Ma, Y.; Nguyen, T. Deposition of highly cross-linked fluorinated amorphous carbon film and structural evolution during thermal annealing. *Appl. Phys. Lett.* **1998**, *73* (11), 1514−1516.

(17) Ma, Y.; Yang, H.; Guo, J.; Sathe, C.; Agui, A.; Nordgren, J. Structural and electronic properties of low dielectric constant fluorinated amorphous carbon films. *Appl. Phys. Lett.* **1998**, *72* (25), 3353−3355.

(18) Yokomichi, H.; Hayashi, T.; Masuda, A. Changes in structure and nature of defects by annealing of fluorinated amorphous carbon thin films with low dielectric constant. *Appl. Phys. Lett.* **1998**, *72* (21), 2704−2706.

10.1021/la051801o CCC: $33.50
Published on Web 01/05/2006

deposition (ICP−CVD),[27,28] magnetron sputtering deposition,[29−32] and ion beam deposition.[33−35] The deposition parameters that influence the properties of *a*-CF_x films are known to include the carbon-to-fluorine elemental ratio in the film, the radio frequency power used in deposition, the process pressure, and the substrate temperature.[17,33,36] The composition of the gas mixture used to deposit the *a*-CF_x film is known to influence the fluorine content in the film[28,37−41] and its deposition rate.[8,19,24,28,38,39,42,43] Increasing the fluorocarbon-to-hydrocarbon ratio in the gas mixture increases both the fluorine content in the film and the deposition rate.

The influence of the fluorine content of *a*-CF_x films on their wetting, tribological, mechanical, structural, and thermal properties has been widely studied. *a*-CF_x films are hydrophobic, and the wetting nature of *a*-CF_x films has been investigated by contact angle measurements. Increasing the fluorine content reduces surface wettability (or surface energy) and is manifested by an increasing contact angle with water.[9,10,20,21,44] It has been suggested that this is due to an increase in the density of CF_n groups on the film surface.[10,20,21]

Fluorine incorporation into carbon films is known to significantly influence their tribological, mechanical, and structural properties. Increasing fluorine content leads to gradual reduction of the friction, adhesion,[7,8,21,45] hardness,[7,8,10,20,25,38,39,41,45] stress,[7,10,33,38] elastic modulus,[20,41] and density of the film.[33,39] A series of hardness tests, stress tests, and density measurements of *a*-CF_x films revealed that the diamond-like structure of carbon films with very low fluorine content is transformed into a graphite-like structure and then a polymer-like structure as the fluorine content of the film is increased.[7,20,33,38] X-ray photoelectron spectroscopy (XPS) analysis of *a*-CF_x films further supports this model by revealing that the fraction of CF_2 and CF_3 groups increases as the fluorine content of the film increases.[20,24,28,29,31,33] Raman spectra exhibit a gradual increase in the intensities of the D bands relative to those of the G bands as the fluorine content of the film increases, revealing the structural change of the film from a diamond-like to a graphite-like and then a polymer-like structure.[20,24,25,33,38,39,46]

Increasing the fluorine content of *a*-CF_x films leads to a reduction of their thermal stability.[33] Conversely, thermal annealing of *a*-CF_x films causes a reduction of their fluorine content, leading to an increase of their thermal stability.[16,27] This is believed to arise from thermal release of fluorine atoms from an *a*-CF_x film, allowing cross-linking of neighboring carbon atoms, which makes the film more thermally stable. The thermal stability of *a*-CF_x films has been reported sporadically and is known to be influenced significantly by the method of film growth,[32,33] the substrate temperature (or deposition temperature),[17,29,47,48] and the fluorine-to-carbon ratio of the gas mixture.[33]

High hardness and thermal stability combined with low wettability, low friction, and low adhesion are desirable properties for the protective carbon overcoats used on data storage media. Unfortunately, improvements of the wetting and tribological properties of amorphous carbon films with increasing fluorine content are achieved at the expense of lowering their mechanical strength and thermal stability. It remains a challenge to find conditions for production of protective coatings with optimal mechanical, thermal, nonwetting, and tribological properties.

(19) Endo, K.; Tatsumi, T. Fluorinated amorphous carbon thin films grown by plasma enhanced chemical vapor deposition for low dielectric constant interlayer dielectrics. *J. Appl. Phys.* **1995**, *78* (2), 1370−1372.

(20) Yu, G. Q.; Tay, B. K.; Sun, Z.; Pan, L. K. Properties of fluorinated amorphous diamond like carbon films by PECVD. *Appl. Surf. Sci.* **2003**, *219*, 228−237.

(21) Prioli, R.; Jacobsohn, L. G.; Maia da Costa, M. E. H.; Freire, F. L., Jr. Nanotribological properties of amophous carbon−fluorine films. *Tribol. Lett.* **2003**, *15* (3), 177−180.

(22) Donnet, C.; Fontaine, J.; Grill, A.; Patel, V.; Jahnes, C.; Belin, M. Wear-rsistant fluorinated diamondlike carbon films. *Surf. Coat. Technol.* **1997**, *94*−*95*, 531−536.

(23) Muller, U.; Hauert, R.; Oral, B.; Tobler, M. Temperature stability of fluorinated amorphous hydrogenated carbon films. *Surf. Coat. Technol.* **1995**, *76*−*77*, 367−371.

(24) Valentini, L.; Braca, E.; Kenny, J. M.; Fedosenko, G.; Engemann, J.; Lozzi, L.; Santucci, S. Analysis of the role of fluorine content on the thermal stability of C:H:F thin films. *Diamond Relat. Mater.* **2002**, *11*, 1100−1105.

(25) Bottani, C. E.; Lamperti, A.; Nobili, L.; Ossi, P. M. Structure and mechanical properties of PACVD fluorinated amorphous carbon films. *Thin Solid Films* **2003**, *433*, 149−154.

(26) Shieh, J.-M.; Tsai, K.-C.; Suen, S.-C.; Dai, B.-T. Improvements of characteristics of fluorinated dielectric films integrated as interlayer dielectrics. *J. Vac. Sci. Technol. B* **2002**, *20* (4), 1388−1393.

(27) Han, S.-S.; Bae, B.-S. Thermal Stability of Fluorinated Amorphous Carbon Thin Films with Low Dielectric Constant. *J. Electrochem. Soc.* **2001**, *148* (4), F67−F72.

(28) Han, S.-S.; Kim, H. R.; Bae, B.-S. Deposition of Fluorinated Amorphous Carbon Thin Films as a Low-Dielectric-Constant Material. *J. Electrochem. Soc.* **1999**, *146* (9), 3383−3388.

(29) Chang, J. P.; Krautter, H. W.; Zhu, W.; Opila, R. L.; Pai, C. S. Integration of fluorinated amorphous carbon as low-dielectric constant insulator: Effects of heating and deposition of tantalum nitride. *J. Vac. Sci. Technol. A* **1999**, *17* (5), 2969−2974.

(30) Trippe, S. C.; Mansano, R. D. Study of fluorine addition influence in the dielectric constant of dimond-like carbon thin film deposited by reactive sputtering. *Mod. Phys. Lett. B* **2002**, *16* (15), 577−582.

(31) Jung, H.-S.; Park, H.-H. Structural and electrical properties of co-sputtered fluorinated amorphous carbon film. *Thin Solid Films* **2002**, *420*−*421*, 248−252.

(32) Yokomichi, H.; Masuda, A. Effects of double bonding configurations on thermal stability of low-hydrogen condentration fluorinated amorphous carbon thin-films with low dielectric constant prepared by sputtering with hydrogen dilution. *Vacuum* **2000**, *59*, 771−776.

(33) Ronning, C.; Buttner, M.; Vetter, U.; Feldermann, H.; Wondratschek, O.; Hofsass, H. Ion beam deposition of fluorinated amorphous carbon. *J. Appl. Phys.* **2001**, *90* (8), 4237−4245.

(34) Karis, T. E.; Tyndall, G. W.; Fenzel-Alexander, D. Ellipsometric measurement of solid fluorocarbon film thickness on magnetic recording media. *J. Appl. Phys.* **1997**, *81* (8), 5378−5379.

(35) Karis, T. E.; Tyndall, G. W.; Fenzel-Alexander, D. Characterization of a solid fluorocarbon film on magnetic recording media. *J. Vac. Sci. Technol. A* **1997**, *15* (4), 2382−2387.

(36) Shieh, J.-M.; Suen, S.-C.; Tsai, K.-C.; Dai, B.-T.; Wu, Y.-C.; Wu, Y.-H. Characteristics of fluorinated amorphous carbon films and implementation of 0.15 μm Cu/*a*-C:F damascene interconnection. *J. Vac. Sci. Technol. B* **2001**, *19* (3), 780−787.

(37) Wang, X.; Harris, H.; Temkin, H.; Gangopadhyay, S.; Strathman, M. D.; West, M. Determination of oscillator strength of C−F vibrations in fluorinated amorphous-carbon films by infrared spectroscopy. *Appl. Phys. Lett.* **2001**, *78* (20), 3079−3081.

(38) Jacobsohn, L. G.; Franceschini, D. F.; Maia da Costa, M. E. H.; Freire, F. L., Jr. Structural and mechanical characterization of fluorinated amorphous-carbon films deposited by plasma decomposition of CF_4−CH_4 gas mixtures. *J. Vac. Sci. Technol. A* **2000**, *18* (5), 2230−2238.

(39) Valentini, L.; Braca, E.; Kenny, J. M.; Lozzi, L.; Santucci, S. Relationship between the opitical and mechanical properties of fluorinated amorphous carbon thin films. *J. Non-Crystalline Solids* **2001**, *291*, 153−159.

(40) d'Agostino, R.; Lamendola, R.; Favia, P. Fluorinated diamondlike carbon films deposited from radio frequency glow discharge in a triode reactor. *J. Vac. Sci. Technol. A* **1994**, *12* (2), 308−313.

(41) Ko, H. J.; Lee, K.-M.; Lee, H.-J.; Yu, Y. H.; Choi, C. K. Mechanical properties of low-*k a*-C:F films by inductively coupled plasma chemical vapor deposition. *J. Korean Phys. Soc.* **2003**, *42*, S952−S955.

(42) Endo, K.; Tatsumi, T. Fluorinated amorphous carbon thin films grown by helicon plasma enhanced chemical vapor deposition for low dielectric constant interlayer dielectrics. *Appl. Phys. Lett.* **1996**, *68* (20), 2864−2866.

(43) Yu, X.; Sheng-Hua, X.; Zhao-Yuan, N.; Xin-Hua, L.; Mei-Fu, J.; Song, H.; Wei, D.; Jun, C.; Chao, Y.; Shan-Hua, C. An *a*-C:F:H film with high-thermal stability by electron cyclotron resonance chemical vapor deposition at room temperature. *Chin. Phys. Lett.* **2003**, *20* (3), 423−426.

(44) Kasai, H.; Kogoma, M.; Moriwaki, T.; Okazaki, S. Surface structure estimation by plasma fluorination of amorphous carbon, diamond, graphite and plastic film surfaces. *J. Phys. D: Appl. Phys.* **1986**, *19*, L225−L228.

(45) Ayala, P.; Maia da Costa, M. E. H.; Prioli, R.; Freire F. L., Jr. Nano- and microscale wear of fluorinated carbon films. *Surf. Coat. Technol.* **2004**, *182*, 335−341.

(46) Lampeti, A.; Ossi, P. M. Systematic study of amorphous hydrogenated and fluorinated carbon films. *Appl. Surf. Sci.* **2003**, *205*, 113−120.

(47) Ariel, N.; Eizenberg, M.; Wang, Y.; Murarka, S. P. Deposition temperature effect on thermal stability of fluorinated amorphous carbon films utilized as low-K dielectrics. *Mater. Sci. Semiconductor Process.* **2001**, *4*, 383−391.

(48) Yang, S.-H.; Park, J.; Kim, J.-Y.; Lee, Y.-K.; Cho, B.-R.; Park, D.-K.; Lee, W. H.; Park, J.-W. Effect of deposition temperature on low-dielectric fluorinated amorphous carbon films for ultralarge-scale integration multilevel interconnects. *Microchem. J.* **1999**, *63*, 161−167.

Fundamental studies of *a*-CF_x films are needed to support the effort to optimize their properties.

Perfluoropolyalkyl ethers (PFPEs) have been used widely as commercial hard disk lubricants because of their chemical stability, high thermal stability, excellent lubricity, low viscosity, and extremely low volatility at high molecular weights. Thus, a PFPE film as thin as 5−20 Å effectively lubricates the disk surface for periods of years without decomposing or evaporating. Fomblin Zdol is one of the common PFPE lubricants and has the chemical structure

$$HOCH_2CF_2-(OCF_2)_x-(OCF_2CF_2)_y-OCF_2CH_2OH$$

where the ratio x/y is typically between $^2/_3$ and 1. Fomblin Zdol has a perfluorinated ether backbone that is terminated by hydroxyl groups at both ends. The interactions of the ether linkages and the hydroxyl-terminal groups of Fomblin Zdol with the surfaces of carbon overcoats influence its properties as a lubricant.

The goal of the work reported in this article has been to probe the interactions of typical PFPE lubricants with the surfaces of *a*-CF_x films. The complex structure of Fomblin Zdol hinders the fundamental study of its interaction with amorphous carbon surfaces. In this report, the terminal hydroxyl groups and ether linkages were emulated by short-chain fluorinated alcohols and ethers, respectively. The interactions between *a*-CF_x films and alcohols [ethanol (CH_3CH_2OH) and 2,2,2-trifluoroethanol (CF_3CH_2OH)] or ethers {diethyl ether [$(CH_3CH_2)_2O$] and perfluorodiethyl ether [$(CF_3CF_2)_2O$]} were investigated using temperature-programmed desorption (TPD). The desorption energies of the alcohols and ethers were measured as a function of coverage to study the interaction of the lubricant backbone and endgroups with the *a*-CF_x surface. Comparisons of the heats of adsorption of the hydrocarbon and fluorocarbon species were used to probe the mechanism of interaction with the overcoat surface.

2. Experimental Section

The carbon films were produced and analyzed in one ultrahigh vacuum (UHV) deposition chamber and then transferred to a second UHV chamber for the studies of alcohol and ether adsorption and desorption. Fluorinated amorphous carbon films were prepared on nickel substrates by dc magnetron sputtering using a graphite target and a mixture of Ar and CF_4 gases. The nickel substrates were cleaned by several cycles of Ar^+ sputtering followed by annealing to 950 K before *a*-CF_x film deposition. Films were then deposited using a dc power of 75 W at a substrate temperature of 443 K (170 °C). The total pressure was maintained at 8 mTorr during the deposition process using a 10% $CF_4/(Ar + CF_4)$ gas mixture. The *a*-CF_x film was characterized by in situ XPS immediately after deposition and then after exposure to air for 1 h at room temperature. The XP spectra were obtained using a Specs 290 W Mg Kα ($h\nu$ = 1253.6 eV) source and a VG Scientific CLAM II hemispherical analyzer. A pass energy of 10 eV was used for all measurements. The film thickness was determined to be about 70 Å from the attenuation of the Ni substrate signal. The film had a fluorine-to-carbon ratio (F/C) of 1.1. A 1-h exposure of the *a*-CF_x film to air increased the oxygen content of the film to ∼5%. The air-exposed surface was then used for subsequent temperature-programmed desorption (TPD) studies and thermal stability measurements.

The sample was taken from the deposition chamber and mounted to a sample holder by spot welding tantalum wires to the nickel substrate. The sample holder was then attached to the end of a manipulator capable of *x*, *y*, and *z* translations and 360° rotation. The manipulator was mounted to a stainless steel UHV chamber with a base pressure below 4×10^{-10} Torr that was achieved using an ion pump and a titanium sublimation pump. Within the chamber, the film could be cooled to 100 K and heated resistively to >1000 K. Leak valves were used to introduce vapors into the chamber for adsorption on the *a*-CF_x film surface. The chamber is equipped with an ABB Extrel Merlin quadrupole mass spectrometer (QMS) with a mass range of 1−500 amu used for TPD studies.

Adsorption of model compounds onto the *a*-CF_x surface was accomplished by leaking vapor into the UHV chamber while the sample was held at 100 K. Ethanol [(CH_3CH_2OH), Aldrich, 99.5%], 2,2,2-trifluoroethanol [(CF_3CH_2OH), TCI-GR], diethyl ether [$(CH_3CH_2)_2O$, Aldrich, 99.9%], and perfluorodiethyl ether [$(CF_3CF_2)_2O$, Strem Chemical, 90%] were each placed in glass vials attached to the leak valve. Any high-vapor-pressure contaminants were removed with several freeze−pump−thaw cycles, and the vapor purity was then checked with mass spectrometry. Exposure of the sample surface to each adsorbate was conducted by positioning the *a*-CF_x sample held at 100 K directly in front of a stainless steel dosing tube that was attached to the leak valve. The distance between the sample and the end of dosing tube was approximately 3 cm. The exposure pressure was maintained at $1-2 \times 10^{-9}$ Torr for variable periods of time.

After adsorption of the vapor, the *a*-CF_x sample was positioned ∼2 mm from the aperture of the mass spectrometer. TPD spectra were obtained by heating the sample at a constant rate of 2 K/s while monitoring the desorbing species with the QMS. To prevent any irreversible damage to the sample during heating, the upper temperature was limited to 315 K, well below the temperature at which the *a*-CF_x film was deposited. The TPD spectra were highly reproducible, indicating that the *a*-CF_x film surface was unchanged by adsorption and desorption of the ethers and alcohols.

The adsorbate coverage was calibrated using desorption spectra obtained from a single-crystal Cu(100) surface that had the same apparent surface area as the *a*-CF_x film. The copper sample was cleaned by multiple cycles of Ar^+ ion sputtering with annealing to 1000 K. The crystalline order of the Cu(100) surface was checked using low-energy electron diffraction (LEED). Thermal desorption spectra of each adsorbate obtained from the Cu(100) surface exhibited clearly resolved monolayer and multilayer desorption features. The peak areas under the monolayer desorption features were determined for each adsorbate and used to calibrate the initial coverages of the adsorbates desorbing from the *a*-CF_x film.

3. Results and Discussion

3.1. Properties of *a*-CF_x Films. *a*-CF_x films were deposited on nickel surfaces by dc magnetron sputtering. The chemical compositions of the *a*-CF_x film were determined by XPS immediately after deposition and then after 1 h of exposure to air (Figure 1). The features appearing at 284.4, 286.8, 289.2, and 291.7 eV have been assigned to C 1s photoemission from C atoms unattached to fluorine and then CF, CF_2, and CF_3 groups, respectively.[16,33] The fluorine-to-carbon ratio was F/C = 1.1 and was not influenced by exposure to air. The feature at 532.7 eV is assigned to O 1s photoelectrons. Although the fresh film did have some residual oxygen, exposure to air resulted in a film with an oxygen content of ∼5%.

The *a*-CF_x film was heated from 100 to 1000 K at a constant rate of 2 K/s to study its decomposition kinetics. The decomposition of the film was studied using a mass spectrometer to monitor the desorption of various species yielding a variety of ionization fragments: H_2^+ ($m/q = 2$), CH_3^+ ($m/q = 15$), F^+ ($m/q = 19$), HF^+ ($m/q = 20$), CF^+ ($m/q = 31$), F_2^+ ($m/q = 38$), and CF_3^+ ($m/q = 69$) (Figure 2). The earliest onset of decomposition and desorption of species into the gas phase occurs at a temperature of $T \approx 450$ K. The onset of rapid decomposition occurs at ∼600 K, and the decomposition rate peaked at $T_p = 700$ K. The activation energy for the decomposition of the fluorocarbon film, $\Delta E^{\ddagger}_{dec}$, was calculated using Redhead's equation

$$\frac{\Delta E^{\ddagger}_{dec}}{RT_p^{\,2}} = \frac{\nu_{dec}}{\beta} \exp\left(\frac{-\Delta E^{\ddagger}_{dec}}{RT_p}\right)$$

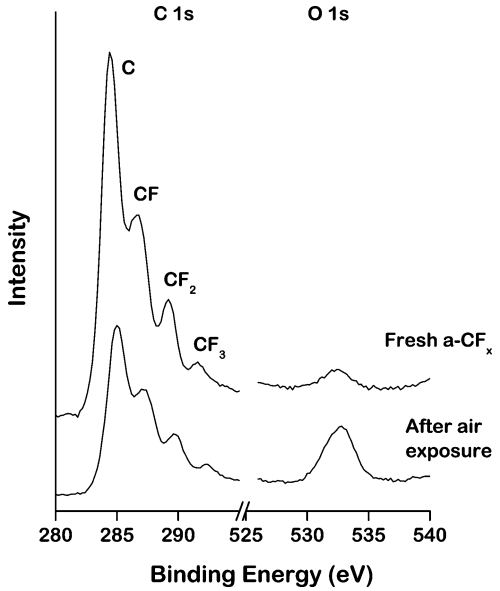

Figure 1. C 1s and O 1s X-ray photoemission spectra of *a*-CF_x obtained immediately after deposition and after a 1-h exposure to air. The C 1s peaks reveal the presence of several partially fluorinated species. Exposure to air results in the oxidation of the film to a level of ~5% oxygen content.

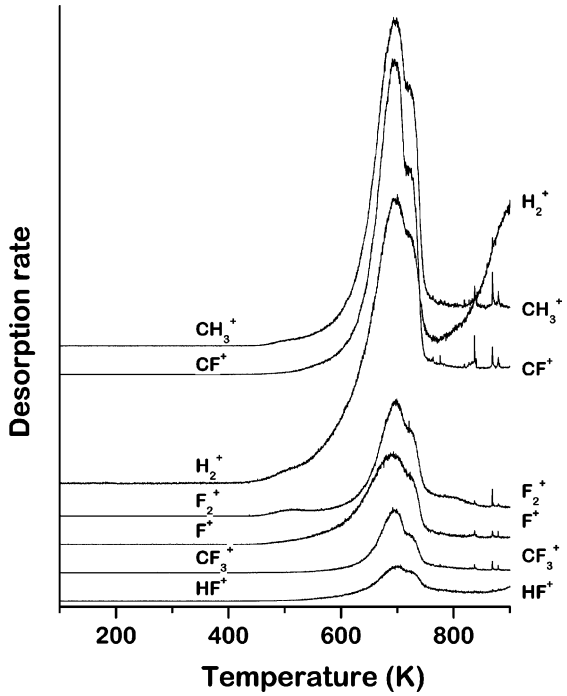

Figure 2. Temperature-programmed decomposition spectra of an *a*-CF_x film during heating at 2 K/s. The presence of hydrogen-containing fragments indicates the presence of some amount of hydrogen in the film. The peak decomposition rate occurs at ~700 K.

where β is the heating rate, ν_{dec} is the preexponential factor, T_p is the peak desorption temperature, and R is the gas constant. This analysis assumes that the preexponential factor has a value of $\nu_{dec} = 10^{13}\ s^{-1}$ and yields a value of $\Delta E^{\ddagger}_{dec} = 190$ kJ/mol from the peak desorption temperature of $T_p = 700$ K.

3.2. Ether Desorption from *a*-CF_x Films. The lubricants used most commonly on hard disk surfaces by the data storage industry are perfluoropolyalkyl ethers (PFPEs). The most common types have fluorinated ether backbones with hydroxyl endgroups and are known by the trade names Fomblin Zdol and Fomblin

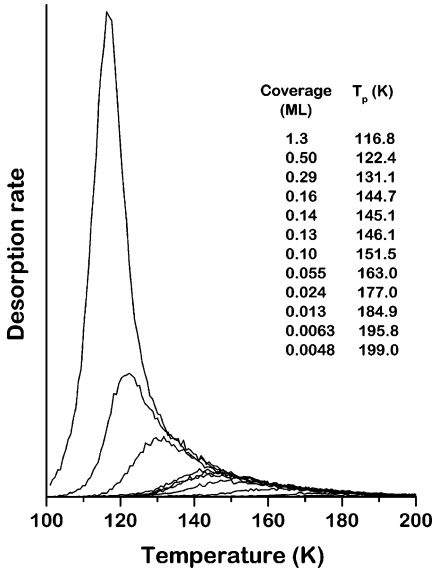

Figure 3. Temperature-programmed desorption spectra of $(CH_3CH_2)_2O$ from the surface of an *a*-CF_x film at initial coverages varying from <1% of a monolayer to > 1 ML. The peak desorption temperatures decrease with increasing coverage. The coverages were calibrated using the area under the $(CH_3CH_2)_2O$ monolayer desorption feature from a Cu(100) surface with the same apparent area as the *a*-CF_x film. The TPD spectra shown were collected using a heating rate of 2 K/s while monitoring the signal at $m/q = 59$ for $(CH_3CH_2)_2O$. Additional spectra were obtained by monitoring the signals at m/q ratios of 2 (H_2^+), 15 (CH_3^+), 29 ($CH_3CH_2^+$), 30 (H_2CO^+), 43 (CH_3CO^+), 45 ($CH_3CH_2O^+$), and 59 ($CH_3CH_2OCH_2^+$) and indicate that $(CH_3CH_2)_2O$ desorbs molecularly.

Ztetraol. Small ethers, i.e., $(CH_3CH_2)_2O$ and $(CF_3CF_2)_2O$, have been used as models for the ether linkages in the Fomblin-based PFPE lubricants. The adsorption and desorption of these compounds from the surfaces of amorphous carbon films can be used to probe the interactions of the ether backbone with the surfaces of amorphous carbon overcoats. Previous studies have shown that the surfaces of amorphous carbon films expose carbon atoms with different hybridization (sp^2 and sp^3) and carbon atoms that are partially oxidized. In other words, the surfaces of these films are chemically heterogeneous.[49,50] The surface heterogeneity of an *a*-CF_x film is revealed by the TPD spectra of simple adsorbates such as alcohols and ethers. Figure 3 shows TPD spectra of $(CH_3CH_2)_2O$ adsorbed on the *a*-CF_x film at coverages ranging from <0.01 ML to >1 ML. The peak desorption temperature shifts monotonically from high to low temperatures with increasing initial coverage, indicating that the desorption energy, ΔE_{des}, decreases with increasing coverage. These desorption curves are qualitatively similar to those observed for other amorphous carbon films.[51−53] The origin of the shift in desorption temperature with increasing coverage is that $(CH_3CH_2)_2O$ molecules first adsorb on the sites with the highest affinity for adsorption and additional molecules then adsorb on the sites with lower affinity. It is worth noting that this heterogeneity might be intrinsic to the surface structure and composition of the *a*-CF_x film or could be influenced by adsorption and the

(49) Cornaglia, L.; Gellman, A. J. Fluoroether bonding to carbon overcoats. *J. Vac. Sci. Technol. A* **1997**, *15* (5), 2755−2765.
(50) McFadden, C. F.; Gellman, A. J. Ultrahigh Vacuum Boundary Lubrication of the Cu−Cu Interface by 2,2,2-Trifluoroethanol. *Langmuir* **1995**, *11* (1), 273−280.
(51) Shukla, N.; Gellman, A. J.; Gui, J. The Interaction of CF_3CH_2OH and $(CF_3CF_2)_2O$ with Amorphous Carbon Films. *Langmuir* **2000**, *16*, 6562−6568.
(52) Paserba, K.; Shukla, N.; Gellman, A. J.; Gui, J.; Marchon, B. Bonding of Ethers and Alcohols to *a*-CN_x Films. *Langmuir* **1999**, *15*, 1709−1715.
(53) Shukla, N.; Gellman, A. J. Interaction of alcohols with *a*-CH_x films. *J. Vac. Sci. Technol. A* **2000**, *18* (5), 2319−2326.

interactions of the adsorbates with the exposed surface. The coverage-dependent peak desorption temperatures observed for amorphous carbon films could, in principle, be due to coverage-dependent repulsive interactions between $(CH_3CH_2)_2O$ molecules adsorbed on the surface. As the coverage increases, these repulsive interactions would decrease the differential desorption energy. This possibility can be ruled out, however, on the basis of studies of $(CH_3CH_2)_2O$ desorption from the homogeneous surface of single-crystalline graphite.[54] Those measurements revealed desorption peak temperatures that increase slightly with increasing coverage, suggesting that the intrinsic interactions between adsorbed $(CH_3CH_2)_2O$ molecules are, if anything, weakly attractive.

As a consequence of the heterogeneity of *a*-CF_x surfaces, there is no clear resolution between monolayer and multilayer desorption features as is commonly observed for homogeneous single-crystalline surfaces such as graphite.[54] The peak desorption temperature decreases smoothly with increasing coverage until the onset of multilayer desorption is reached. As a consequence, the coverage of the adsorbed layer is difficult to calibrate because it is not possible to determine the coverage corresponding to a monolayer. To calibrate the coverage for all the compounds used in this study, desorption spectra were obtained from a homogeneous Cu(100) surface. The measurements made use of a Cu(100) single crystal that had the same apparent surface area as the *a*-CF_x sample. The spectra (not shown) for all four ethers and alcohols used in this work exhibited a clear resolution of the monolayer desorption feature at higher temperature and the multilayer desorption feature at lower temperature, indicating that the Cu(100) surface is truly homogeneous. The peak area under the monolayer region was measured and was used to calibrate the adsorbate coverage desorbing from the *a*-CF_x film.

Effects of Fluorination on the Adsorption of Alcohols and Ethers on *a*-CF_x Films. Fluorination of alcohols and ethers influences their interactions with the surface of the *a*-CF_x film and can be used to probe the mechanism of their interaction with amorphous carbon films. Desorption of $(CH_3CH_2)_2O$ and $(CF_3CF_2)_2O$ from the *a*-CF_x film was used to model the interaction of the ether backbones of the Fomblin lubricants with the surface. The desorption spectra of $(CF_3CF_2)_2O$ from the *a*-CF_x film are shown in Figure 4 for comparison with those of $(CH_3CH_2)_2O$ shown in Figure 3. The fragmentation patterns of the desorbing species indicate that both desorb from the surface molecularly without undergoing decomposition. Both sets of desorption spectra also show a monotonic decrease in the peak desorption temperature with increasing coverage. Closer examination of the $(CH_3CH_2)_2O$ and $(CF_3CF_2)_2O$ desorption spectra reveals that the peak desorption temperatures of $(CF_3CF_2)_2O$ fall significantly below those of $(CH_3CH_2)_2O$, suggesting that the interaction of $(CF_3CF_2)_2O$ with the surface is weaker than that of $(CH_3CH_2)_2O$.

The interactions of the end groups of Fomblin Zdol and Ztetraol with the surface of the *a*-CF_x film were probed by studying the desorption kinetics of CH_3CH_2OH and CF_3CH_2OH from the *a*-CF_x film (Figures 5 and 6). Desorption spectra were obtained while monitoring a number of different ionization fragments for each alcohol and indicate that both desorb molecularly without undergoing decomposition on the *a*-CF_x surface. This is consistent with the results of all previous studies of these compounds on the surfaces of *a*-CH_x, *a*-CN_x, and graphite.[51−54] As with the ethers, the desorption spectra of both CH_3CH_2OH and CF_3CH_2OH show that their peak desorption temperatures decrease monotonically as the coverage increases from 0 to 1 ML. These results reflect the heterogeneity of the *a*-CF_x surface.

The TPD spectra of the ethers and alcohols on the *a*-CF_x surface can be used to estimate their desorption energies as a function of coverage. Comparison of the desorption energies of (CH_3-

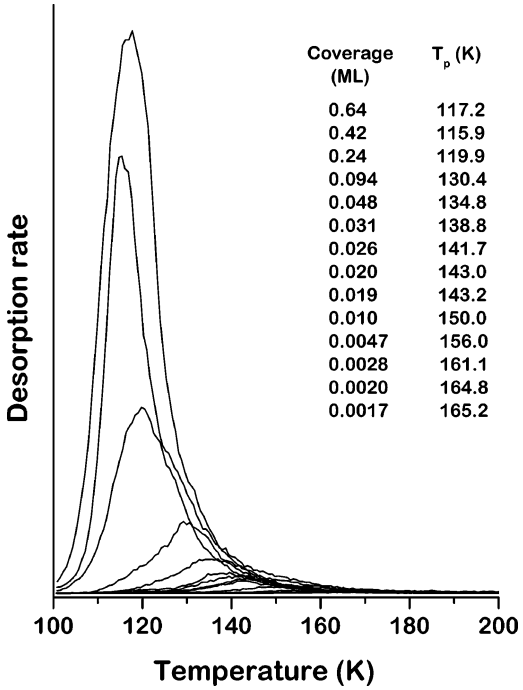

Figure 4. Temperature-programmed desorption spectra of $(CF_3CF_2)_2O$ from the surface of an *a*-CF_x film at initial coverages varying from <0.01 to 0.64 ML. The peak desorption temperatures decrease with increasing coverage. The TPD spectra shown were collected using a heating rate of 2 K/s while monitoring the signal at m/q = 69 for $(CF_3CF_2)_2O$. Additional spectra were obtained by monitoring the signals at m/q ratios of 19 (F^+), 66 (F_2CO^+), 69 (CF_3^+), 97 (CF_3CO^+), 119 ($CF_3CF_2^+$), 135 ($CF_3CF_2O^+$), and 185 ($CF_3CF_2OCF_2^+$). These indicate that $(CF_3CF_2)_2O$ desorbs molecularly.

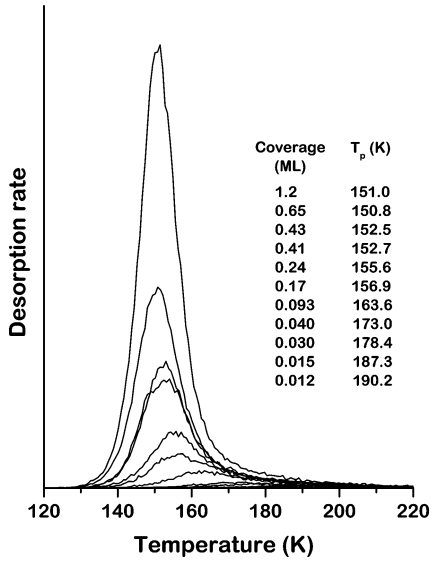

Figure 5. Temperature-programmed desorption spectra of CH_3CH_2OH from the surface of an *a*-CF_x film at initial coverages varying from <0.01 to >1 ML. The peak desorption temperature decreases with increasing coverage. The TPD spectra were collected using a heating rate of 2 K/s while monitoring the signal at m/q = 31. Additional desorption spectra were obtained by monitoring the signals at m/q ratios of 15 (CH_3^+), 28 ($CH_2CH_2^+$), 29 (CHO^+), 30 ($CH_3CH_3^+$), 31 (CH_2OH^+), 43 (CH_3CO^+), and 45 ($CH_3CH_2O^+$). These indicate that CH_3CH_2OH desorbs molecularly.

(54) Shukla, N.; Gui, J.; Gellman, A. J. Adsorption of Fluorinated Ethers and Alcohols on Graphite. *Langmuir* **2001**, *17*, 2395−2401.

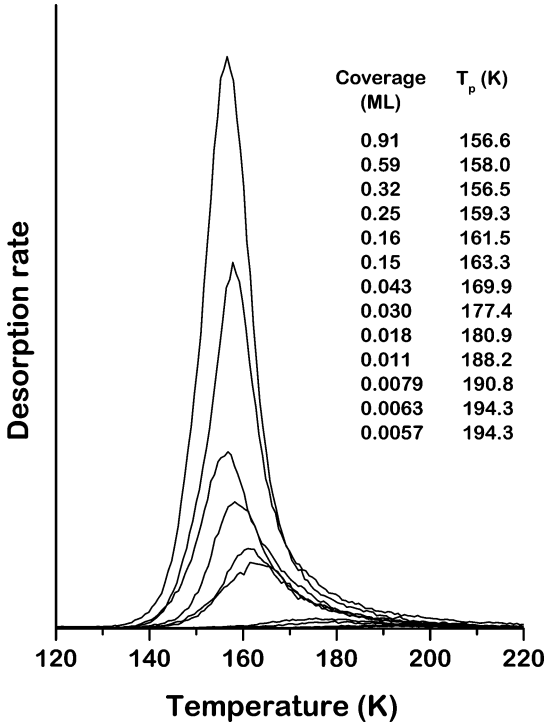

Figure 6. Temperature-programmed desorption spectra of CF_3CH_2OH from the surface of an *a*-CF_x film at initial coverages varying from <0.01 to 0.91 ML. The peak desorption temperature decreases with increasing coverage. The TPD spectra were collected using a heating rate of 2 K/s while monitoring the signal at $m/q = 31$. Additional desorption spectra were obtained by monitoring the signals at m/q ratios of 19 (F^+), 31 (CH_2OH^+), 50 (CF_2^+), 69 (CF_3^+), 83 ($CF_3CH_2^+$), 84 ($CF_3CH_3^+$), and 100 ($CF_3CH_2OH^+$). These indicate that CF_3CH_2OH desorbs molecularly.

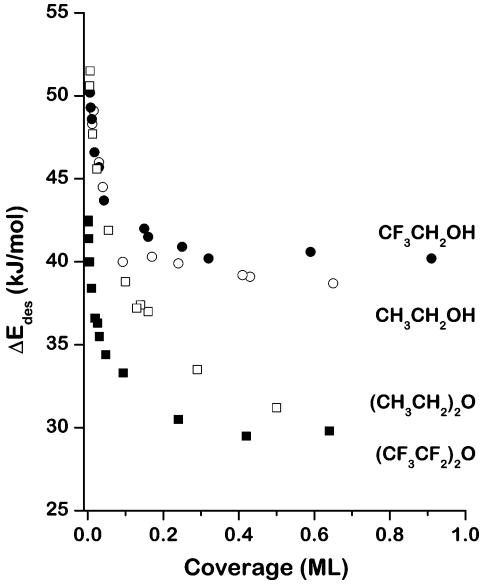

Figure 7. Desorption energies of CH_3CH_2OH (○), CF_3CF_2OH (●), $(CH_3CH_2)_2O$ (□), and $(CF_3CF_2)_2O$ (■) from *a*-CF_x films as functions of coverage. These energies all decrease monotonically with increasing coverage, reflecting the heterogeneity of the *a*-CF_x surface. Whereas fluorination of the diethyl ether decreases its desorption energy, fluorination of the ethanol has no significant effect on its desorption energy.

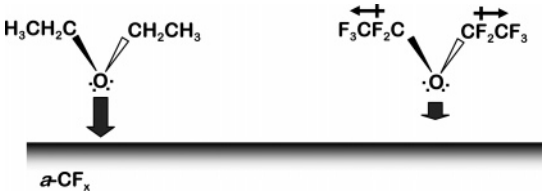

Figure 8. Proposed models for the interaction of diethyl ether and perfluorodiethyl ether with *a*-CF_x films. Ethers bind to the *a*-CF_x surface through a dative bond formed by electron donation from oxygen lone-pair electrons to the film. Fluorination of the diethyl ether increases the magnitude of the local dipoles on the ethyl groups and destabilizes the partial positive charge induced on oxygen by electron donation, leading to a reduction of its desorption energy.

$CH_2)_2O$ with those of $(CF_3CF_2)_2O$ and the desorption energies of CH_3CH_2OH with those of CF_3CH_2OH provides some insight into the nature of the interaction of the hydroxyl groups and ether linkages of Fomblin Zdol with the *a*-CF_x surface. The desorption energies were estimated using Redhead's equation with a preexponential factor of $\nu_{des} = 10^{13}$ s^{-1}. Because the intent of this investigation was to compare the desorption energies of the fluorocarbons with those of the hydrocarbons, errors in the assumed magnitude of the desorption preexponent are not important. The desorption energies of CH_3CH_2OH, CF_3CH_2OH, $(CH_3CH_2)_2O$ and $(CF_3CF_2)_2O$ adsorbed on the *a*-CF_x film are shown in Figure 7 as a function of coverage. As expected on the basis of the coverage dependence of the peak desorption temperatures, the desorption energies decrease monotonically with increasing coverage. Consistent with all previous measurements of this type, we also observe that the desorption energies of the alcohols are higher than those of the ethers.

In previous work, the mechanism of interaction of alcohols and ethers with amorphous carbon films has been probed by comparing the desorption energies of hydrocarbon and fluorocarbon ethers. Previous work on *a*-CH_x[53] and *a*-CN_x[52] films found that, in the limit of zero coverage, the desorption energies of CF_3CH_2OH were ~5 kJ/mol higher than those of CH_3CH_2OH. The interpretation of those results was that, at the sites with highest affinity for alcohol adsorption, the alcohols interact with the surface via hydrogen bonding. Fluorination of the alcohol tends to increase the strength of hydrogen bonding. In contrast, our measurements of the desorption energies of CH_3CH_2OH and CF_3CH_2OH from the surface of *a*-CF_x show no significant difference for coverages up to ~0.1 ML. The origin of the differences in alcohol adsorption on these *a*-CF_x films and that on the *a*-CH_x and *a*-CN_x films is not clear.

The desorption energies of $(CH_3CH_2)_2O$ from the *a*-CF_x surface are significantly different from those of $(CF_3CF_2)_2O$ at submonolayer coverage. As the coverages approach zero, the difference between desorption energies of $(CH_3CH_2)_2O$ and $(CF_3CF_2)_2O$ reaches ~9 kJ/mol. Previous studies observed the same trend for ether desorption from *a*-CH_x and *a*-CN_x surfaces. On *a*-CH_x surfaces, the desorption energy of $(CH_3CH_2)_2O$ is higher than that of $(CF_3CF_2)_2O$.[49] The desorption energy of $(CH_3CH_2)_2O$ is ~10 kJ/mol higher than that of $(CF_3CF_2)_2O$ on *a*-CN_x surfaces.[52] The fact that fluorination decreases the ether's desorption energy suggests that ethers bind to the *a*-CF_x surface through a dative bond formed by donation of the lone-pair electrons on the oxygen atom. This binding mechanism and the effect of fluorination are depicted in Figure 8. Substitution of fluorine into an ether increases the magnitude of the local dipole moments on the ethyl groups and destabilizes the partial positive charge induced on oxygen by electron donation. The net effect of fluorination on the interaction through the dative bond is a reduction of the desorption energy of the ether.

A TPD study of alcohols and ethers was conducted with an *a*-CH_x film for comparison with the results obtained from the *a*-CF_x film. This *a*-CH_x film was prepared in the same apparatus

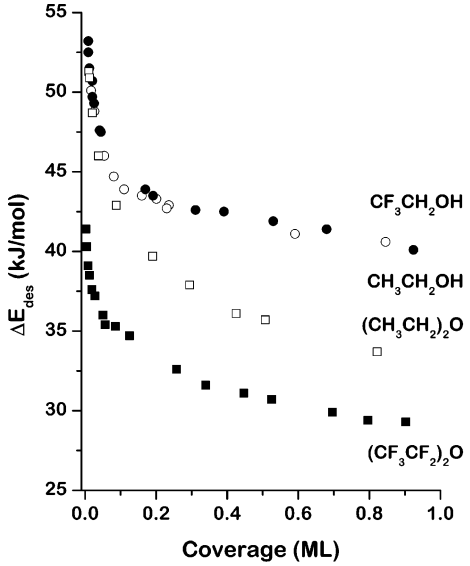

Figure 9. Desorption energies of CH_3CH_2OH (○), CF_3CF_2OH (●), $(CH_3CH_2)_2O$ (□), and $(CF_3CF_2)_2O$ (■) from *a*-CH_x films as functions of coverage. These energies all decrease monotonically with increasing coverage, reflecting the heterogeneity of the *a*-CH_x surface. Whereas fluorination of the diethyl ether decreases its desorption energy, fluorination of the ethanol has no significant effect on its desorption energy.

as the *a*-CF_x film using the same deposition conditions but substituting CH_4 for CF_4. Once deposited, it was transferred from the deposition chamber to the TPD chamber through air. The same experimental procedures and data analysis methods were applied to the desorption study on the *a*-CH_x film. The desorption energies of CH_3CH_2OH, CF_3CH_2OH, $(CH_3CH_2)_2O$, and $(CF_3CF_2)_2O$ from *a*-CH_x are shown in Figure 9 as a function of coverage. As for the *a*-CF_x surface, the desorption energy of $(CH_3CH_2)_2O$ at low coverage is ∼10 kJ/mol higher than that of $(CF_3CF_2)_2O$. Close examination of Figures 7 and 9 reveals that the magnitude of the desorption energies of the alcohols and ethers and the ranges of their values are similar for both the *a*-CH_x and *a*-CF_x films. The desorption energies of $(CH_3CH_2)_2O$ are 2−5 kJ/mol lower for the a-CF_x film than for the *a*-CH_x film. For both surfaces, the desorption energies of the fluorinated ethers are significantly lower than those of the hydrocarbon ethers. The general behavior of the ethers on these surfaces is the same as was observed in previous studies of *a*-CH_x and *a*-CN_x surfaces.[49,52] The data are all consistent with a model for the interaction of the ether with the amorphous carbon films in which a dative bond is formed via donation of electrons from the oxygen atom (Figure 8).

The desorption energies of CH_3CH_2OH and CF_3CH_2OH from the *a*-CH_x and *a*-CF_x surfaces have the same magnitude and range. The desorption energies for the *a*-CF_x surface are ∼2 kJ/mol lower than those for the *a*-CH_x surface. One of the interesting features of these data is that, for both surfaces, the desorption energy of CH_3CH_2OH is the same as that of CF_3CH_2OH. In previous work on *a*-CH_x and *a*-CN_x films at low coverages, the desorption energies of fluorinated alcohols were found to be higher than those of the corresponding hydrocarbon alcohols. This has been taken to suggest that alcohols interact with these surfaces via hydrogen bonding. The current data do not show this difference between CH_3CH_2OH and CF_3CH_2OH. One reason for the difference might be the difference in the method of defining coverage between this and previous studies. In this study, the coverage of each adsorbate on both *a*-CH_x and *a*-CF_x films was calibrated using desorption from the Cu(100) surface, for which the monolayer desorption peak is well-defined and resolved from the multilayer desorption feature. This method of defining coverage is viable because the carbon films and the Cu(100) surface have the same apparent surface area. In previous studies, however, the coverage was calibrated by defining the monolayer as the coverage at which one observes the onset of zeroth-order desorption kinetics characteristic of multilayer desorption.[51,53] This is less precise and can differ among different molecules. Thus, the current data call into question the previous proposal that alcohols interact with amorphous carbon surfaces via hydrogen bonding.

The desorption energies of small ethers and alcohols should, in principle, provide some insight into the desorption energies of long-chain perfluoropolyalkyl ether lubricants with hydroxyl endgroups; however, the connection is somewhat indirect. The only direct measurements of the desorption energies of long-chain (>1000 amu) Fomblin Zdol lubricants from surfaces were made on single-crystalline graphite.[55] At some level, the desorption energy of a long polymeric chain such as a Fomblin from a surface must be dictated by the interactions of its individual monomer units with the surface. It is important, however, to appreciate that the effective desorption energy that one determines from measurements of desorption kinetics is a not a direct measure of the true desorption energy as defined at 0 K. The kinetics of polymer desorption are heavily influenced by conformational entropy effects that must be taken into consideration.[56−58]

4. Conclusions

The surface properties of an amorphous fluorinated carbon film (*a*-CF_x) have been studied using XPS, temperature-programmed annealing, and the adsorption and desorption of small hydrocarbon and fluorocarbon ethers and alcohols used to model the segments in the PFPE lubricants commonly used on the surfaces of hard disks. An *a*-CF_x film with a fluorine-to-carbon composition ratio of 1.1 exhibited an onset of thermal decomposition at ∼450 K and then rapid decomposition at ∼600 K. Thermal desorption of $(CH_3CH_2)_2O$, $(CF_3CF_2)_2O$, CH_3CH_2-OH, and CF_3CH_2OH revealed reversible molecular adsorption on *a*-CF_x. The desorption spectra also revealed the heterogeneity of the *a*-CF_x and a monotonic decrease in the desorption energies of all four compounds as their coverages increase from 0 to 1 ML. Fluorination of the ether reduces its desorption energy, suggesting that ethers bond to the *a*-CF_x surface via a dative interaction with the lone-pair electrons on the oxygen atom. Fluorination of the alcohol does not have a significant effect on its desorption energy.

Acknowledgment. Funding for this work was provided by the Information Storage Industry Consortium (INSIC) and the Heat Assisted Magnetic Recording (HAMR) program support by the U.S. Department of Commerce, National Institute of Standards and Technology, Advanced Technology Program, Cooperative Agreement Number 70NANB1H3056.

LA051801O

(55) Paserba, K. R.; Gellman, A. J. Desorption Kinetics and Energetics of Monodisperse Fomblin Zdol from Carbon Surfaces. *J. Phys. Chem. B* **2001**, *105* (48), 12105−12110.

(56) Paserba, K. R.; Gellman, A. J. Effects of conformational isomerism on the desorption kinetics of *n*-alkanes from graphite. *J. Chem. Phys.* **2001**, *115* (4), 6737−6751.

(57) Paserba, K. R.; Gellman, A. J. Kinetics and Energetics of Oligomer Desorption from Surfaces. *Phys. Rev. Lett.* **2001**, *106* (19), 13231−13241.

(58) Paserba, K. R.; Vaidyanathan, N.; Gellman, A. J. Conformational Entropy Effects on the Desorption Kinetics of Polyethers from Graphite. *Langmuir* **2002**, *18* (25), 9799−9809.